

PHOTOPRODUCTION OFF NUCLEI AND POINT-LIKE PHOTON INTERACTIONS

Part I: Cross Sections and Nuclear Shadowing

R. Engel

*Universität Leipzig, Fachbereich Physik, D-04109 Leipzig, Germany
and Universität Siegen, Fachbereich Physik, D-57068 Siegen, Germany*

J. Ranft

*Departamento de Física de Partículas, Universidade de Santiago de Compostela,
E-15706 Santiago de Compostela, Spain*

and

S. Roesler

Universität Siegen, Fachbereich Physik, D-57068 Siegen, Germany

Abstract

High energy photoproduction off nuclear targets is studied within the Glauber-Gribov approximation. The photon is assumed to interact as a $q\bar{q}$ -system according to the Generalized Vector Dominance Model and as a “bare photon” in direct scattering processes with target nucleons. We calculate total cross sections for interactions of photons with nuclei taking into account coherence length effects and point-like interactions of the photon. Results are compared to data on photon-nucleus cross sections, nuclear shadowing, and quasi-elastic ρ -production. Extrapolations of cross sections and of the shadowing behaviour to high energies are given.

Siegen SI 96-09
Santiago de Compostela US-FT/42-96
October, 1996

1 Introduction

During the last years, the understanding of photon-hadron interactions has considerably improved due to new experimental data from photoproduction and low- x measurements in ep collisions at HERA and due to their interpretation in terms of QCD-inspired multiple-interaction models [1]. Experimental evidence for the classification of photon interactions within the parton model into *direct* and *resolved* interactions has been found [2, 3]. Both classes of processes show different features concerning cross sections as well as multiparticle production [4, 5].

Within the QCD-improved parton model, in direct processes the photon couples directly to a parton of the hadron, whereas in resolved processes it enters the scattering process as a hadronic quark-antiquark fluctuation. Resolved processes are well described in the framework of the Generalized Vector Dominance Model (GVDM) (see for example [6, 7] and references therein). Due to relatively large lifetimes the $q\bar{q}$ -states may develop properties of ordinary hadrons by emitting and absorbing virtual partons. Therefore, the $q\bar{q}$ -states can either interact with the hadron in soft scattering processes (the produced final-state particles have small transverse momenta) or the partons of the $q\bar{q}$ -system can participate in hard interactions with the partons of the hadron [8, 9]. In case of a hard interaction and if the mass of the $q\bar{q}$ -fluctuation is large in comparison to the perturbative QCD scale Λ_{QCD} , it is possible to calculate not only the hard parton-parton scattering but also the splitting of the photon into the $q\bar{q}$ -pair perturbatively. These hard resolved interactions of high-mass $q\bar{q}$ -states are frequently called *anomalous* photon interactions [10].

Here, we want to study the implications of the above mentioned experimental findings on direct and resolved processes to the understanding of photon-nucleus collisions at comparable or higher photon energies.

High energy photon-nucleus collisions have been studied experimentally and theoretically by numerous groups (for recent reviews we refer to [11, 12]). It was found that they bear a remarkable resemblance to hadron-nucleus interactions. For instance, both show decreasing per-nucleon cross sections with increasing nucleus mass number, an effect which is known as “shadowing”. Again, the GVDM provides a natural interpretation of these photon-hadron similarities [6, 7]. Like in hadron-nucleus collisions, shadowing in photon-nucleus collisions can then be described in the framework of the Gribov-Glauber approximation [13, 14, 15]. It relates the total photon-nucleus cross section to effective $q\bar{q}$ -nucleon cross sections [12, 16, 17, 18, 19]. However, the application of the Gribov-Glauber formalism to the multiple scattering process of a $q\bar{q}$ -state without further constraints is only justified if the interaction length exceeds the nuclear radius [20]. This is not the case for the above mentioned direct processes since the photon interacts in such processes with only one nucleon. As we will argue further below, at high energies it might also be not the case for anomalous photon interactions. In particular, we will consider the extreme assumption that the interaction time is less than any internucleon distance, i.e. that again only one target nucleon is involved. For these reasons, in the following we call direct and anomalous photon interactions *point-like* processes. They may lead to a suppression of the Glauber-multiple scattering process, i.e. to a suppression of shadowing. It can be expected that this feature is most clearly pronounced in photon scattering processes off heavy nuclei and at high energies, where the cross section of the point-like photon-nucleon interaction becomes sizeable as compared to the total photon-nucleon cross section.

The intention of the present paper is twofold: calculating cross sections of photon-nucleus interactions we (i) investigate the influence of point-like processes on the shadowing behaviour at high energies and (ii) provide the basis for a forthcoming study of particle production in photon-nucleus collisions [21]. In Sect. 2 we consider photon-nucleon collisions and derive total cross sections for $q\bar{q}$ -nucleon interactions. In Sect. 3 point-like photon interactions are discussed and their contribution to the total photon-nucleon cross section is estimated. In Sect. 4 we calculate photon-nucleus cross sections and the shadowing behaviour. Both are compared to data on photoproduction and Deep Inelastic Scattering (DIS) off nuclei and extrapolations to high energies are given. Finally, in Sect. 5 we summarize our results.

2 Total photon-nucleon cross sections

Throughout this paper we consider the photon-nucleon scattering process in the laboratory-frame (nucleon rest frame) using the following kinematical variables. The Bjorken- x variable is defined as $x = Q^2/2m\nu$ denoting with Q^2 , ν , and m the photon virtuality, the photon energy, and the nucleon mass, resp. The squared total energy of the photon-nucleon system is given by $s = Q^2(1-x)/x + m^2$. We restrict our discussions to small x -values ($x < 0.1$) and to the limit $s \gg Q^2$.

Within the diagonal GVDM [6, 7] it is assumed that the virtual photon fluctuates into intermediate $q\bar{q}$ -states V of mass M which subsequently may interact with the nucleon N . This fact can be expressed by a spectral relation of the form [7, 12, 22]

$$\sigma_{\gamma^*N}(s, Q^2) = 4\pi\alpha_{\text{em}} \int_{M_0^2}^{M_1^2} dM^2 D(M^2) \left(\frac{M^2}{M^2 + Q^2} \right)^2 \left(1 + \epsilon \frac{Q^2}{M^2} \right) \sigma_{VN}(s, Q^2, M^2). \quad (1)$$

We use $\alpha_{\text{em}} = e^2/4\pi = 1/137$. The factor $D(M^2)$ incorporates the density of $q\bar{q}$ -systems per unit mass-squared interval:

$$D(M^2) = \frac{R_{e^+e^-}(M^2)}{12\pi^2 M^2}, \quad R_{e^+e^-}(M^2) = \frac{\sigma_{e^+e^- \rightarrow \text{hadrons}}(M^2)}{\sigma_{e^+e^- \rightarrow \mu^+\mu^-}(M^2)} \approx 3 \sum_f e_f^2, \quad (2)$$

where we sum up the squared quark charges of all quark flavors being energetically accessible. ϵ is the ratio between the fluxes of longitudinally and transversally polarized photons. σ_{VN} denotes the effective cross section for the interaction of a $q\bar{q}$ -system with mass M with a nucleon.

Considering low- Q^2 γ^*p scattering only, a detailed model for the M^2 - and Q^2 -dependence of σ_{VN} is not needed. At high collision energies, the average lifetime of the hadronic $q\bar{q}$ -fluctuation $t_f \sim 2\nu/(M^2 + Q^2)$ is almost always larger than the typical hadronic interaction time t_{int} (for nucleons $t_{\text{int}} \sim r_N \approx 1$ fm). However, in photon-nucleus collisions the M^2 - and Q^2 -dependence of σ_{VN} might be important since the coherence length $d \sim t_f$ of the hadronic fluctuation can become comparable to or smaller than the nuclear radius or the nuclear mean free path ($\approx 1/(n\sigma_{VN})$, with n being the number of nucleons per unit volume) [7]. Therefore, in the following we are going to estimate the (purely theoretical) quantity σ_{VN} using Eq.(1) and a parametrization for the experimentally measurable cross section σ_{γ^*N} .

With increasing mass M of the $q\bar{q}$ -system the virtuality of the q and \bar{q} of the system increases. As a consequence the transverse size of the hadronic fluctuation and, hence, σ_{VN} decreases like $1/M^2$ at large M^2 [7, 19]. Following Ref. [7] we approximate this effect parametrizing σ_{VN} as

$$\sigma_{VN}(s, Q^2, M^2) = \frac{\tilde{\sigma}_{VN}(s, Q^2)}{M^2 + Q^2 + C^2}. \quad (3)$$

Here, C is a model-dependent parameter [7] and taken to be $C^2 = 2 \text{ GeV}^2$. With Eq.(3) the M^2 -dependence of the integrand in Eq.(1) is explicitly known and the integration over M^2 between $M_0^2 = 4m_\pi^2$ and $M_1^2 = s$ can be performed. The lower integration limit corresponds to the kinematical threshold. Alternatively, the contributions from the low mass vector mesons ρ^0 , ω , and ϕ could be added as separate terms to the continuum (Eq.(1)), in this case starting the integration at m_ϕ^2 [12, 23]. However, this has been omitted for simplicity. The upper limit, here formally taken to be s , has practically no influence on the results at low and moderate Q^2 since high M^2 -values are suppressed. The only quantity on the r.h.s. of Eqs.(1,3) which is unknown so far is $\tilde{\sigma}_{VN}$. Using a parametrization for σ_{γ^*N} , the M^2 -independent part of Eq.(3), $\tilde{\sigma}_{VN}$, can be calculated for each value of s and Q^2 .

Applying the convention of Ref. [24], the cross section for the scattering of virtual photons off nucleons σ_{γ^*N} can be written as

$$\sigma_{\gamma^*N}(s, Q^2) = \frac{4\pi^2\alpha_{\text{em}}}{Q^2(1-x)} F_2^N(x, Q^2). \quad (4)$$

Since in the present paper we want to study cross sections and shadowing in the Q^2 -region of both, photoproduction and DIS, we use the model of Capella *et al.* [25] (CKMT model) for the structure function F_2^N which provides a simple analytical parametrization valid for $0 \leq Q^2 \lesssim 5 \text{ GeV}^2$. The nucleon structure function is derived from Regge arguments taking rescattering effects into account:

$$F_2^N(x, Q^2) = Ax^{-\Delta(Q^2)}(1-x)^{n(Q^2)+4} \left(\frac{Q^2}{Q^2+a} \right)^{1+\Delta(Q^2)} + B x^{1-\alpha_R}(1-x)^{n(Q^2)} \left(\frac{Q^2}{Q^2+b} \right)^{\alpha_R} \quad (5)$$

with

$$\Delta(Q^2) = \Delta_0 \left(1 + \frac{2Q^2}{Q^2+d} \right), \quad n(Q^2) = \frac{3}{2} \left(1 + \frac{Q^2}{Q^2+c} \right). \quad (6)$$

The first term in (5) is associated with the pomeron contribution determining the small- x behaviour of the sea-quark distribution function whereas the second term is parametrized according to secondary reggeon contributions governing the valence-quark distribution function of the nucleon. We refer to [25] for the values of the parameters entering the expressions. The structure function resulting from this model is in reasonable agreement with measurements [25]. Using the ansatz for the gluon distribution as given in [25] we obtain F_2^N for higher values of Q^2 by performing a QCD evolution in leading logarithmic approximation.

We note that also other parametrizations would be suitable, for instance the parametrization of Abramowicz *et al.* [26] and in the low Q^2 -range the parametrizations of Badelek and Kwieciński [27]. Furthermore, for low values of Q^2 the photon-nucleon cross section σ_{γ^*N}

can be equally well obtained in the framework of the two-component Dual Parton Model (DPM) [8, 9]. The advantage of the two-component DPM calculation is that in this case a detailed model for the inelastic final states exists [9], which we will also apply to the study of particle production in a forthcoming paper [21].

In Fig. 1 we compare the photoproduction cross sections $\sigma_{\gamma p}^{\text{tot}}$ obtained from the CKMT-model (thick solid line) and calculated within the two-component DPM (dotted line) with data [28, 29, 30]. The differences in the high energy extrapolation reflect the typical size of the theoretical uncertainties.

In Fig. 2 a) we show the energy-dependence of the effective cross section σ_{VN} for $M^2 = m_\rho^2$ and different Q^2 values. As observed in γ^*p collisions, the rise of the cross section with energy becomes steeper with increasing photon virtuality. In Fig. 2 b) the Q^2 -dependence of σ_{VN} for different energies and $M^2 = m_\rho^2$ is given. As expected, the Q^2 dependence is very weak for $Q^2 < m_\rho^2 + C^2$.

3 Contributions from point-like interactions of the photon

It should be emphasized that resolved as well as direct photon interactions are included in the description of photon-nucleon scattering via the GVDm (Eq.(1)). Of course, a sharp distinction between direct and resolved interactions is not possible. In direct interactions, the photon couples directly to a parton of the nucleon which determines the highest virtuality of the scattering process (see Fig. 3 a). In resolved interactions, the photon may fluctuate into a $q\bar{q}$ -pair with high virtuality. For example, a $q\bar{q}$ -system can emit a gluon leading to a quark with even higher virtuality which couples to a gluon of the nucleon as shown in Fig. 3 b). Therefore, it is necessary to distinguish two scales to characterize a hard photon-nucleon scattering: (i) the virtuality M of the hadronic $q\bar{q}$ -fluctuation and (ii) the scale of the hard scattering μ which is approximately given by the momentum transfer in the hard scattering process. Then, for $\mu^2 \approx M^2$ the interaction is classified as direct interaction whereas for $\mu^2 \gg M^2$ the interaction is a resolved one. As already mentioned, in case of resolved interactions with $\mu^2 \gg M^2$ and $M^2 \gg \Lambda_{\text{QCD}}^2$, not only the hard parton-parton scattering but also the splitting of the photon into the $q\bar{q}$ -pair can be calculated perturbatively. These interactions lead to a rise of the photon structure function with μ^2 like $\ln(\mu^2)$ (anomalous contribution to the photon structure function [10]). In the following we consider as point-like photon interactions all processes which are characterized by $M^2 \gg \Lambda_{\text{QCD}}^2$ [31].

In direct and anomalous processes either M^2 or the transverse momentum of the hard scattering, p_\perp , acts as hard scale permitting perturbative calculations. Therefore, the cross section for direct processes $\sigma_{\gamma^*N}^{\text{dir}}$ and the cross section $\sigma_{\gamma^*N}^{\text{ano}}$ for the fluctuation of a photon into a $q\bar{q}$ -system with a large mass M (i.e. highly virtual quarks) and the interaction of this system with a nucleon can be estimated using perturbative QCD.

In lowest-order perturbative QCD, the direct photon-nucleon cross section follows from

$$\sigma_{\gamma^*N}^{\text{dir}}(s, p_\perp^{\text{cutoff}}) = \int dx d\hat{t} \sum_{i,k,l} f_{i|N}(x, \mu^2) \frac{d\sigma_{\gamma,i \rightarrow k,l}^{\text{QCD}}(\hat{s}, \hat{t})}{d\hat{t}} \Theta(p_\perp - p_\perp^{\text{cutoff}}), \quad (7)$$

where $f_{i|N}$ denotes the parton distribution function (PDF) for the parton i of the nucleon and the sum runs over all possible parton configurations (i, k, l) . For the calculation we use $\mu^2 = p_\perp^2/4$. The transverse momentum cutoff p_\perp^{cutoff} restricts the integration to the perturbatively reliable region.

In order to calculate the anomalous cross section $\sigma_{\gamma^*N}^{\text{ano}}$, we use the PHOJET Monte Carlo (MC) event generator [8, 9] to simulate hard resolved photon-nucleon interactions according to the cross section

$$\sigma_{\gamma N}^{\text{res}}(s, p_\perp^{\text{cutoff}}) = \int dx_1 dx_2 d\hat{t} \sum_{i,j,k,l} \left(\frac{1}{1 + \delta_{k,l}} f_{i|\gamma}(x_1, \mu^2) f_{j|N}(x_2, \mu^2) \times \frac{d\sigma_{i,j \rightarrow k,l}^{\text{QCD}}(\hat{s}, \hat{t})}{d\hat{t}} \Theta(p_\perp - p_\perp^{\text{cutoff}}) \right). \quad (8)$$

This cross section receives contributions from low-mass and high-mass $q\bar{q}$ -fluctuations. In order to determine the cross section due to anomalous interactions, initial state parton showers were generated for each hard interaction using a backwards evolution algorithm similar to the one discussed in [32, 33] using the parton transverse momentum as evolution variable. Some basic coherence effects are implemented by imposing angular ordering of the parton emissions. Furthermore, the possibility to have a hard $\gamma \rightarrow q\bar{q}$ process during the shower evolution is taken into account. After each parton emission, the probability to stop the parton shower evolution due to a point-like splitting is taken to be the ratio of the $\gamma \rightarrow q\bar{q}$ contribution to the quark density in the photon

$$q(x, \mu^2) = \frac{3\alpha_{\text{em}}}{2\pi} e_q^2 \left[(x^2 + (1-x)^2) \ln \left(\frac{1-x}{x} \frac{\mu^2}{(p_\perp^{\text{cutoff}})^2} \right) + 8x(1-x) - 1 \right] \quad (9)$$

and the quark density of the full photon PDF. Since we are only interested in $\gamma \rightarrow q\bar{q}$ splittings with a remnant quark having $p_\perp > p_\perp^{\text{cutoff}}$, the transverse momentum cutoff p_\perp^{cutoff} is used in (9) as the lowest quark virtuality. Then, the fraction of the anomalous cross section to the total hard resolved photon-nucleon cross section is given by the fraction of events where an anomalous splitting with $p_\perp > p_\perp^{\text{cutoff}}$ has been generated. Within the calculations, we use the GRV PDF parametrizations for the photon [34] and the proton [35]. For the transverse momentum cutoff a value of 3 GeV/c is applied consistently to both, direct and resolved interactions. Regarding the choice of this value we refer to a forthcoming paper [21]. In this paper we want to study particle production in photon-nucleus interactions based on the PHOJET-model for the description of photon-nucleon interactions. There, we will argue that a model which should give a reasonable description of photoproduction off nuclei has to be able to describe the main features of photon-proton interactions as well. Since it was found by the H1-Collaboration [4] that the PHOJET event generator provides a reasonable description of γp photoproduction at 200 GeV c.m. energy using a transverse momentum cutoff of 3 GeV/c we use this value consistently for the calculation of cross sections and of particle production in photon-proton and in photon-nucleus interactions. The formalism presented here is only applicable for photons with low Q^2 , i.e. $Q^2 \ll 4p_\perp^2$. In Fig. 1 the calculated cross sections for direct and anomalous photon interactions on a proton target are shown.

4 Photon-nucleus interactions

4.1 Cross sections

The application of Eq.(1) to the scattering of a virtual photon on a nuclear target of mass number A is straightforward (see [12] and references therein). In order to calculate the total virtual photon-nucleus cross section σ_{γ^*A} , σ_{VN} has to be replaced by the effective cross section σ_{VA} for the interaction of a $q\bar{q}$ -system of mass M with a nucleus with mass number A :

$$\sigma_{\gamma^*A}(s, Q^2) = 4\pi\alpha_{\text{em}} \int_{M_0^2}^{M_1^2} dM^2 D(M^2) \left(\frac{M^2}{M^2 + Q^2} \right)^2 \left(1 + \epsilon \frac{Q^2}{M^2} \right) \sigma_{VA}(s, Q^2, M^2). \quad (10)$$

σ_{VA} is obtained as follows: For coherence lengths d of the hadronic fluctuation

$$d = \frac{2\nu}{M^2 + Q^2} \quad (11)$$

exceeding the average distance between two nucleons the $q\bar{q}$ -system may interact coherently with several nucleons of the target nucleus. This multiple scattering process can be described using the MC realization of the Glauber-Gribov approximation by Shmakov *et al.* [36], here, extended to photon projectiles. The high energy small-angle scattering amplitude F for the interaction of a $q\bar{q}$ -system with a nucleus at impact parameter \vec{b} can be written in terms of the impact parameter amplitude Γ for the interaction of the $q\bar{q}$ -system with individual nucleons [36]

$$F(\vec{b}) = \langle \psi_A^f | 1 - \prod_{i=1}^A [1 - \Gamma(\vec{b}_i)] | \psi_A^i \rangle, \quad \vec{b}_i = \vec{b} - \vec{s}_i. \quad (12)$$

The \vec{s}_i are the coordinates of the nucleons with regard to the center of mass of the nucleus in the plane of impact parameter. The scattering amplitude is averaged over the initial and final state wave functions ψ_A^i and ψ_A^f of the nucleus. For the $q\bar{q}$ -nucleon scattering amplitude we assume the following parametrization

$$\Gamma(s, Q^2, M^2, \vec{b}) = \frac{\sigma_{VN}(s, Q^2, M^2)}{4\pi B(s, Q^2, M^2)} \left(1 - i \frac{\Re f(0)}{\Im m f(0)} \right) \exp \left(\frac{\vec{b}^2}{2B(s, Q^2, M^2)} \right). \quad (13)$$

The effective $q\bar{q}$ -nucleon cross section σ_{VN} is obtained as discussed in Sect.2 (Eq.(3)). We adopt the parametrization of the slope B from [37]

$$B(s, Q^2, M^2) = 2 \left[B_0^2 + \alpha'_P \ln \left(\frac{s}{M^2 + Q^2} \right) \right],$$

$$B_0^2 = \left(2 + \frac{m_p^2}{M^2 + Q^2} \right) \text{ GeV}^{-2}, \quad \alpha'_P = 0.25 \text{ GeV}^{-2}, \quad (14)$$

and assume for the ratio $\Re f(0)/\Im m f(0)$ a constant value of 0.1. Neglecting correlations between nucleons one may write

$$|\psi_A^i|^2 = \prod_{j=1}^A \rho_A(\vec{s}_j, z_j), \quad \rho_A(\vec{r}) = \frac{K}{1 + \exp[(|\vec{r}| - R_A)/c]} \quad (15)$$

where ρ_A is the one-particle Woods-Saxon density distribution with $c = 0.545$ fm and $R_A = 1.12A^{1/3}$ fm [38]. Therefore, for the total, inelastic, and elastic $q\bar{q}$ -nucleus cross sections σ_{VA}^{tot} , $\sigma_{VA}^{\text{inel}}$, and σ_{VA}^{el} we obtain

$$\begin{aligned}\sigma_{VA}^{\text{tot}}(s, Q^2, M^2) &= 2\Re \int d^2b F(s, Q^2, M^2, \vec{b}) \\ &= 2\Re \left\{ \int d^2b \int \prod_{j=1}^A d^3r_j \rho_A(\vec{r}_j) \left(1 - \prod_{i=1}^A [1 - \Gamma(s, Q^2, M^2, \vec{b}_i)] \right) \right\},\end{aligned}\quad (16)$$

$$\begin{aligned}\sigma_{VA}^{\text{inel}}(s, Q^2, M^2) &= \int d^2b \left(1 - |1 - F(s, Q^2, M^2, \vec{b})|^2 \right) \\ &= \int d^2b \int \prod_{j=1}^A d^3r_j \rho_A(\vec{r}_j) \left(1 - \left| \prod_{i=1}^A [1 - \Gamma(s, Q^2, M^2, \vec{b}_i)] \right|^2 \right),\end{aligned}\quad (17)$$

$$\sigma_{VA}^{\text{el}}(s, Q^2, M^2) = \sigma_{VA}^{\text{tot}}(s, Q^2, M^2) - \sigma_{VA}^{\text{inel}}(s, Q^2, M^2). \quad (18)$$

The integrations over the \vec{r}_j 's are performed by taking the average of the integrand in Eqs.(16,17) over a sufficiently large number of nucleon coordinates sets sampled from the density distribution ρ_A .

At low energies the coherence length d may lead to a suppression of shadowing which we take into account in the calculation of the product over the A nucleons for a fixed spatial nucleon configuration (Eqs.(16,17)). In the non-shadowing limit, i.e. if d is smaller than any internucleon distance, we obtain a sum over $\Gamma(\vec{b}_i)$ and, therefore, $\sigma_{VA} \approx A\sigma_{VN}$.

As discussed initially, in direct photon interactions the Glauber multiple scattering process is, per definition, completely suppressed since the photon couples directly to a parton in a nucleon without leaving any remnant. In contrast, the assumption that also in anomalous photon interactions the Glauber cascade is reduced to one $q\bar{q}$ -nucleon scattering can only be considered as an extreme case. However, this might be justified since we are interested in estimating the maximum possible effect of the point-like interactions on the shadowing behaviour at high energies. We recognize however, that the soft component of hard processes has been discussed (see for instance [39]). It is obvious, how the point-like processes have to be taken into account in Eq.(13): σ_{VN} has to be replaced by $(1 - \xi)\sigma_{VN}$ and $A \cdot \sigma_{\gamma^*N}^{\text{pl}}$ is added explicitly to Eq.(10), with

$$\xi(s, Q^2) = \frac{\sigma_{\gamma^*N}^{\text{pl}}(s, Q^2)}{\sigma_{\gamma^*N}^{\text{tot}}(s, Q^2)}, \quad \sigma_{\gamma^*N}^{\text{pl}}(s, Q^2) = \sigma_{\gamma^*N}^{\text{dir}}(s, Q^2) + \sigma_{\gamma^*N}^{\text{ano}}(s, Q^2). \quad (19)$$

In Fig. 4 we compare our results on $\sigma_{\gamma A}$ in the photoproduction limit ($Q^2 = 0$) for carbon, copper, and lead targets (solid lines) to data [40, 41, 42, 43]. The agreement is reasonable apart from the low energy region where our results for the carbon target seem to show less shadowing than measured. However, for $\nu \approx 2 - 3$ GeV the lower energy limit of the applicability of the model is reached. In addition, we indicate with dotted lines the cross sections which would be obtained if one neglects the limited coherence length at low energies. Whereas this effect is less significant for light targets, it is responsible for the increase of the cross sections towards lower energies observed in interactions of real photons with copper and lead nuclei.

An extrapolation in energy of the real photon-nucleus cross section is presented in Fig. 5, again, for the three target nuclei carbon, copper, and lead. Here, the point-like interactions lead to a stronger increase of the cross sections above a photon-nucleon c.m. energy of 100 GeV (solid lines) than it would be obtained neglecting the suppression of the Glauber-cascade by point-like processes (dotted lines).

4.2 Nuclear shadowing of photons

The ratio of the total photon-nucleus to the total photon-nucleon cross section, which gives the effective number of nucleons A_{eff} “seen” by the photon projectile, has been measured in photoproduction experiments using carbon, copper, and lead targets [40, 41, 42, 43]. We compare these data in the form A_{eff}/A , frequently called “effective attenuation”, to results of our calculations in Fig. 6a-c. The agreement is reasonable. However, there are considerable uncertainties within the measurements as well as differences between the results obtained in different experiments which make it difficult to draw further conclusions from this comparison.

In Fig. 7 the shadowing ratios $\sigma_{\gamma^*A}/(A\sigma_{\gamma^*N})$ for real photons are extrapolated in energy up to a photon-nucleon c.m. energy of 2 TeV. In order to study the influence of point-like processes to the high energy shadowing behaviour we plot the full model (solid lines) and the cross sections obtained if the point-like processes are not taken into consideration (dotted lines). From this comparison we conclude that point-like processes are responsible for a decrease of the nuclear shadowing with increasing energy.

Let us now turn to lepton-nucleus interactions where the shadowing region ($x < 0.1$) has been investigated by the E665-Collaboration using 470 GeV/ c muons and by the NMC-Collaboration using 200 GeV muons. Within our calculations the flux g of virtual photons is sampled according to the equivalent photon approximation (EPA) folded with the Q^2 -dependent cross section σ_{γ^*A} (Eq.(10), see also [9] for details)

$$\sigma_{lA} = \int dy \int dQ^2 g(y, Q^2) \sigma_{\gamma^*A}(s, Q^2), \quad (20)$$

with y being the lepton energy fraction taken by the photon. The kinematic cuts as they were applied to the measured data are taken into account. In Fig. 8a-c we compare the model predictions concerning the x -dependence of the cross section ratios to E665- [44] and NMC data [45, 46]. Our results are binned in the same way as the E665 data showing that our photon-flux approximation gives average x -values in each bin which correspond to the measured ones. The average Q^2 -values range from 0.15 GeV² in the lowest x -bin up to 7.9 GeV² in the highest bin. The calculations for the three target nuclei carbon, calcium, and lead are in good agreement with the E665 data but overestimate the NMC data slightly.

In order to study the Q^2 -dependence of the cross section ratios at fixed values of x we parametrize them as

$$R^A = \frac{\sigma_{\gamma^*A}}{A\sigma_{\gamma^*N}} = a + b \cdot \log(Q^2/\text{GeV}^2). \quad (21)$$

In Fig. 9 we plot the slope b as function of x , again for carbon, calcium, and lead targets, together with E665-measurements [44]. Our results are consistent with the experimental

observations, i.e. with a weak Q^2 -dependence of the shadowing effect within the considered x -range.

The strength of shadowing may also be studied by parametrizing the per-nucleon cross section ratios by $R^A \propto A^{\alpha-1}$. In Fig. 10 we compare results of our calculations on the values of α to E665 data [44]. Even though our values are systematically above the data, they are still compatible with them.

Extrapolating the shadowing ratios to high energies at fixed large values of Q^2 ($x \rightarrow 0$) Kopeliovich and Povh predicted within their model that shadowing vanishes [47]. As shown in Fig. 11 for carbon (a) and lead targets (b), within our model we predict the same qualitative features since the soft contributions are stronger suppressed with the photon virtuality than the point-like contributions. Applying an energy-independent cutoff to calculate the point-like photon interactions, one would get also a decrease of shadowing in the photoproduction limit at very high energies. However, it is expected that the transverse momentum cutoff should increase with energy in order to guarantee that the calculation is restricted to a kinematic region where lowest-order perturbative QCD estimates are reliable. Several parametrizations of the energy-dependence of the cutoff have been suggested in [48, 49]. These parametrizations predict a only slowly varying cutoff up to c.m. energies of about 2 TeV. Therefore, we assume that the qualitative results reported here do not change applying an energy-dependent cutoff. This has been confirmed numerically for the parametrization discussed in [49].

4.3 Quasi-elastic vector meson production

A further test of the Q^2 -behaviour of our model can be performed by studying quasi-elastic vector meson production. For example, the cross section for the (coherent) quasi-elastic ρ^0 production off a nucleus with mass number A depends on Q^2 like

$$\sigma_{\gamma^* A \rightarrow \rho^0 A}(s, Q^2) \sim \left(\frac{m_\rho^2}{m_\rho^2 + Q^2} \right)^2 \left(1 + \epsilon \frac{Q^2}{m_\rho^2} \right) \sigma_{\rho^0 A}^{\text{el}}(s, Q^2) \quad (22)$$

where $\sigma_{\rho^0 A}^{\text{el}}$ is obtained according to (18). In Fig. 12 we show our results together with data of the NMC-Collab. [50]. In each Q^2 -bin, the average photon energy and the average value of ϵ were used as given in [50]. In order to compare the shape, our results were normalized to the data. Parametrizing $\sigma_{\rho^0 A}^{\text{el}}$ as

$$\sigma_{\rho^0 A}^{\text{el}}(Q^2) = \sigma_0 \left(\frac{Q_0^2}{Q^2} \right)^\beta \quad (23)$$

we get from a fit to our results values for β of 2.6 for deuterium, 2.5 for carbon, and 2.4 for calcium. Since our results slightly deviate from a power-law behaviour in Q^2 we estimate the uncertainties for the β -values by excluding either the cross sections at the two lowest or highest Q^2 from the fit. For the three β -values we obtain an uncertainty of ± 0.2 . Comparing it to the experimental value of $\beta = 2.02 \pm 0.07$ from a combined fit to the data for the three target nuclei [50], we conclude that our results show a somewhat stronger Q^2 -dependence than the NMC data.

5 Summary and conclusions

Cross sections for photon-nucleus interactions are calculated based on the assumption that the photon may interact directly or as a “resolved” $q\bar{q}$ -state. We apply the Generalized Vector Dominance Model together with Glauber-Gribov theory taking coherence length effects into account. Total photon-nucleon cross sections are calculated within the CKMT-model.

We assume that direct and anomalous photon interactions are point-like, i.e. the photon interacts with only one target nucleon. The cross sections corresponding to the point-like processes are estimated within lowest order perturbative QCD. The suppression of the Glauber cascade due to these point-like photon interactions is explicitly taken into account.

Real photon-nucleus cross sections are compared to data and extrapolated to high energies. In addition, we study the shadowing behaviour in photon-nucleus interactions for moderate photon virtualities by comparing them to data. In both cases a good agreement with the data is found. It is discussed that point-like photon interactions lead to a suppressed shadowing in interactions with heavy target nuclei at high energies.

In a forthcoming paper we will extend this study to particle production in interactions of weakly virtual photons off nuclei. There, the description of particle production will be based on the above discussed cross sections and shadowing behaviour combined with the ideas of the two-component Dual Parton Model describing photon-nucleon interactions.

Acknowledgements

Discussions with F. W. Bopp are gratefully acknowledged. One of the authors (J.R.) thanks C. Pajares for the hospitality at the University Santiago de Compostela and he was supported by the Direccion General de Politicia Cientifica of Spain. One of the authors (R.E.) was supported by the Deutsche Forschungsgemeinschaft under contract No. Schi 422/1-2.

References

- [1] M. Erdmann: The Partonic Structure of the Photon: Photoproduction at the Lepton-Proton Collider HERA, DESY 96-090, 1996
- [2] H1 Collab.: T. Ahmed et al.: Phys. Lett. B297 (1992) 205
- [3] ZEUS Collab.: M. Derrick et al.: Phys. Lett. B322 (1994) 287
- [4] H1 Collab.: S. Aid et al.: Z. Phys. C70 (1995) 17
- [5] ZEUS Collab.: M. Derrick et al.: Phys. Lett. B354 (1995) 136
- [6] T. H. Bauer, R. D. Spital and D. R. Yennie: Rev. Mod. Phys. 50 (1978) 261
- [7] G. Grammer, Jr. and D. Sullivan: *Nuclear Shadowing of Electromagnetic Processes*, Plenum Press, New York, 1978 in: Electromagnetic Interactions of Hadrons, Volume 2, ed. by A. Donnachie and G. Shaw
- [8] R. Engel: Z. Phys. C66 (1995) 203
- [9] R. Engel and J. Ranft: Phys. Rev. D54 (1996) 4244
- [10] E. Witten: Nucl. Phys. B120 (1977) 189
- [11] M. Arneodo: Phys. Rep. 240 (1994) 301
- [12] G. Piller, W. Ratzka and W. Weise: Z. Phys. A352 (1995) 427
- [13] R. Glauber: Phys. Rev. 100 (1955) 242
- [14] V. N. Gribov: JETP 30 (1970) 709
- [15] L. Bertochi: Il Nuovo Cimento 11A (1972) 45
- [16] L. L. Frankfurt and M. I. Strikman: Nucl. Phys. B316 (1989) 340
- [17] L. L. Frankfurt, G. A. Miller and M. I. Strikman: Annu. Rev. Nucl. Part. Sci. 45 (1994) 501
- [18] G. V. Davidenko and N. N. Nikolaev: Nucl. Phys. B135 (1978) 333
- [19] B. L. Ioffe, V. A. Khoze and L. N. Lipatov: *Hard Processes, Volume 1: Phenomenology Quark-Parton Model*, North-Holland Physics Publishing, Amsterdam, 1984
- [20] J. Hüfner, B. Kopeliovich and J. Nemchik: Phys. Lett. B383 (1996) 362
- [21] R. Engel, J. Ranft and S. Roesler: Photoproduction off nuclei and point-like photon interactions; Part II: Particle production, in preparation, 1996
- [22] J. J. Sakurai and D. Schildknecht: Phys. Lett. 40B (1972) 121

- [23] B. Gorczyca and D. Schildknecht: Phys. Lett. 47B (1973) 71
- [24] V. M. Budnev, I. F. Ginzburg, G. V. Meledin and V. G. Serbo: Phys. Rep. 15C (1975) 181
- [25] A. Capella, A. Kaidalov, C. Merino and J. Tran Thanh Van: Phys. Lett. B337 (1994) 358
- [26] H. Abramowicz, E. M. Levin, A. Levy and U. Maor: Phys. Lett. B269 (1991) 465
- [27] B. Badelek and J. Kwieciński: Phys. Lett. B295 (1992) 263
- [28] S. I. Alekhin et al.: Compilation of cross sections 4, CERN-HERA 87-01, 1987
- [29] ZEUS Collab.: M. Derrick et al.: Z. Phys. C63 (1994) 391
- [30] H1 Collab.: S. Aid et al.: Z. Phys. C69 (1995) 27
- [31] G. A. Schuler and T. Sjöstrand: Nucl. Phys. B407 (1993) 539
- [32] T. Sjöstrand: Phys. Lett. B157 (1985) 321
- [33] T. Gottschalk: Nucl. Phys. B277 (1986) 700
- [34] M. Glück, E. Reya and A. Vogt: Phys. Rev. D46 (1992) 1973
- [35] M. Glück, E. Reya and A. Vogt: Phys. Rev. D45 (1992) 3986
- [36] S. Y. Shmakov, V. V. Uzhinskii and A. M. Zadoroshny: Comp. Phys. Commun. 54 (1989) 125
- [37] L. P. A. Haakman, A. Kaidalov and J. H. Koch: Phys. Lett. B365 (1996) 411
- [38] E. Segré: *Nuclei and particles* Reading Mass Benjamin 1977
- [39] B. Kopeliovich: Soft Component of Hard Reactions and Nuclear Shadowing, in Proceedings of the Workshop Hirschegg'95: Dynamical Properties of Hadrons in Nuclear Matter, ed. by H. Feldmeier and W. Nörenberg, Darmstadt, p. 102, 1995
- [40] E. A. Arakelyan et al.: Phys. Lett. 79B (1978) 143
- [41] G. R. Brookes et al.: Phys. Rev. D8 (1973) 2826
- [42] D. O. Caldwell et al.: Phys. Rev. D7 (1973) 1362
- [43] D. O. Caldwell et al.: Phys. Rev. Lett. 42 (1979) 553
- [44] E665-Collab.: M. R. Adams et al.: Z. Phys. C67 (1995) 403
- [45] New Muon Collab.: P. Amaudruz et al.: Z. Phys. C51 (1991) 387

- [46] New Muon Collab.: M. Arneodo et al.: Nucl. Phys. B441 (1995) 12
- [47] B. Kopeliovich and B. Povh: Interplay of Soft and Hard Interactions in Nuclear Shadowing at High Q^2 and Low x , MPI H-V28-1996, 1996
- [48] K. Geiger: Phys. Rev. D47 (1993) 133
- [49] F. W. Bopp, R. Engel, D. Pertermann and Ranft: Phys. Rev. D49 (1994) 3236
- [50] New Muon Collab.: M. Arneodo et al.: Nucl. Phys. B429 (1994) 503

Figure Captions

1. Total photon-proton cross sections as calculated with the CKMT-model [25] (thick solid line) and obtained within the two-component DPM (dotted line) are shown together with measurements [28, 29, 30]. In addition, we give the contribution to the total cross section from direct processes and the cross section reflecting the anomalous component of the photon-PDFs.
2. The effective $q\bar{q}$ -nucleon cross sections at $M^2 = m_\rho^2$ are shown. In (a) the dependence on the energy is given for three different photon virtualities. In (b) we show the Q^2 -behaviour for three different energies.
3. Examples for point-like interactions of the photon. In (a) direct photon-nucleon interactions contributing in lowest order p QCD and in (b) an example for an anomalous photon-nucleon interaction are shown.
4. The dependence of the total cross sections for interactions of real photons with carbon, copper, and lead on the photon energy (full lines) is compared to measurements [40, 41, 42, 43]. The influence of the coherence length is indicated by dotted lines where we show the cross sections as they would be obtained disregarding the finite coherence length of the photon.
5. Extrapolation of total cross sections for photoproduction off carbon-, copper-, and lead-nuclei. \sqrt{s} is the photon-nucleon c.m. energy. The pure GVDM-prediction is shown by the dotted lines. The cross sections taking the suppression of shadowing by point-like photon-nucleon interactions into consideration are given by solid lines.
6. Per-nucleon ratios of real photon-carbon (a), -copper (b), and -lead (c) cross sections to photon-nucleon cross sections are shown together with measurements [40, 41, 42, 43].
7. As in Fig. 5 but for the shadowing ratios.
8. The dependence of the per-nucleon ratios of photon-carbon (a), -calcium (b), and -lead (c) cross sections to photon-nucleon cross sections on the Bjorken- x is compared to data of the E665- [44] and NMC-Collab. [45, 46].
9. The slopes of the logarithmic Q^2 -dependence of the shadowing ratio R^A are compared to results of the E665-Collab. [44].
10. The A -dependence of the per-nucleon cross section ratios $R^A \propto A^{\alpha-1}$ for different bins of the Bjorken- x is shown together with E665 data [44].
11. Bjorken- x -dependence of the per-nucleon ratios of photon-carbon (a) and photon-lead (b) cross sections to photon-nucleon cross sections shown for $Q^2 = 0.1, 0.5, 1.0$, and 5.0 GeV^2 (from the bottom to the top).

12. Dependence of the quasi-elastic ρ^0 -production cross sections on the photon virtuality for photon-deuterium (a), -carbon (b), and -calcium (c) interactions. The model results are normalized to the data of the NMC-Collab. [50].

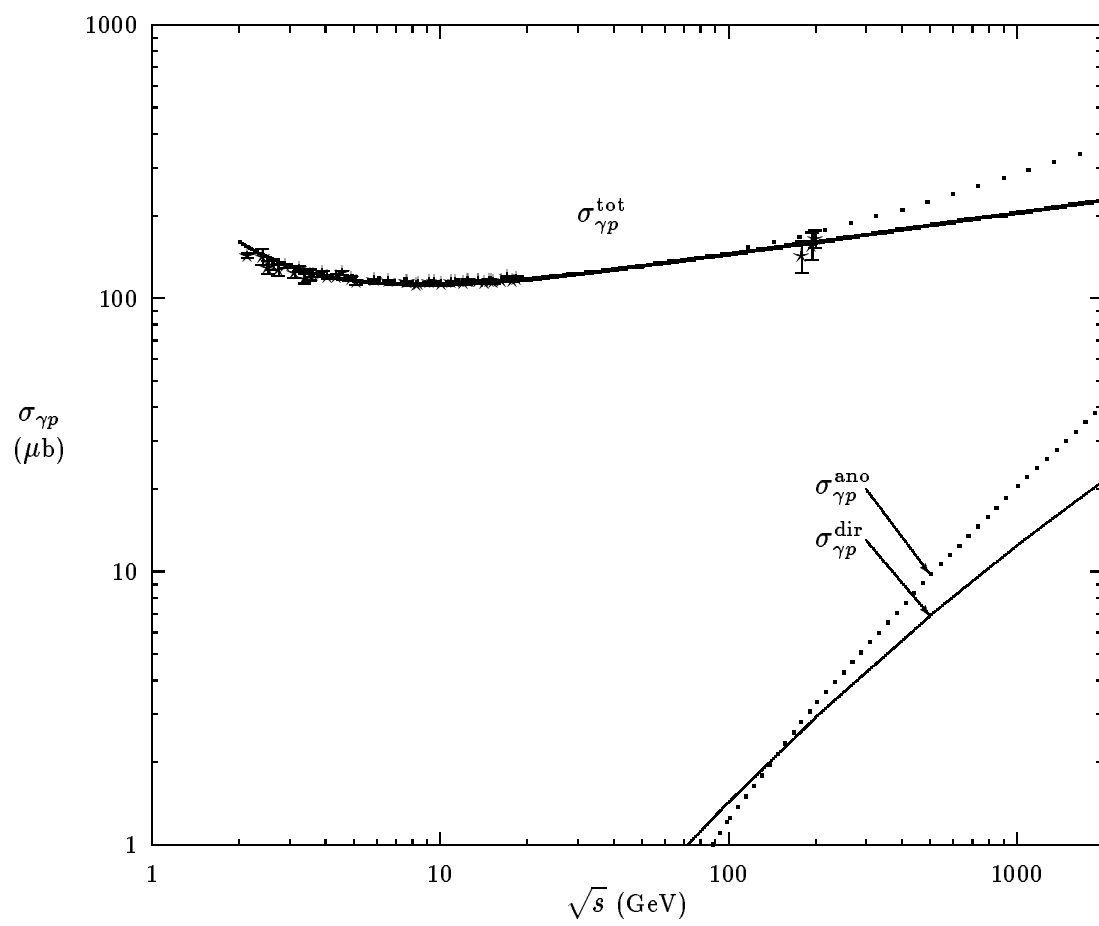
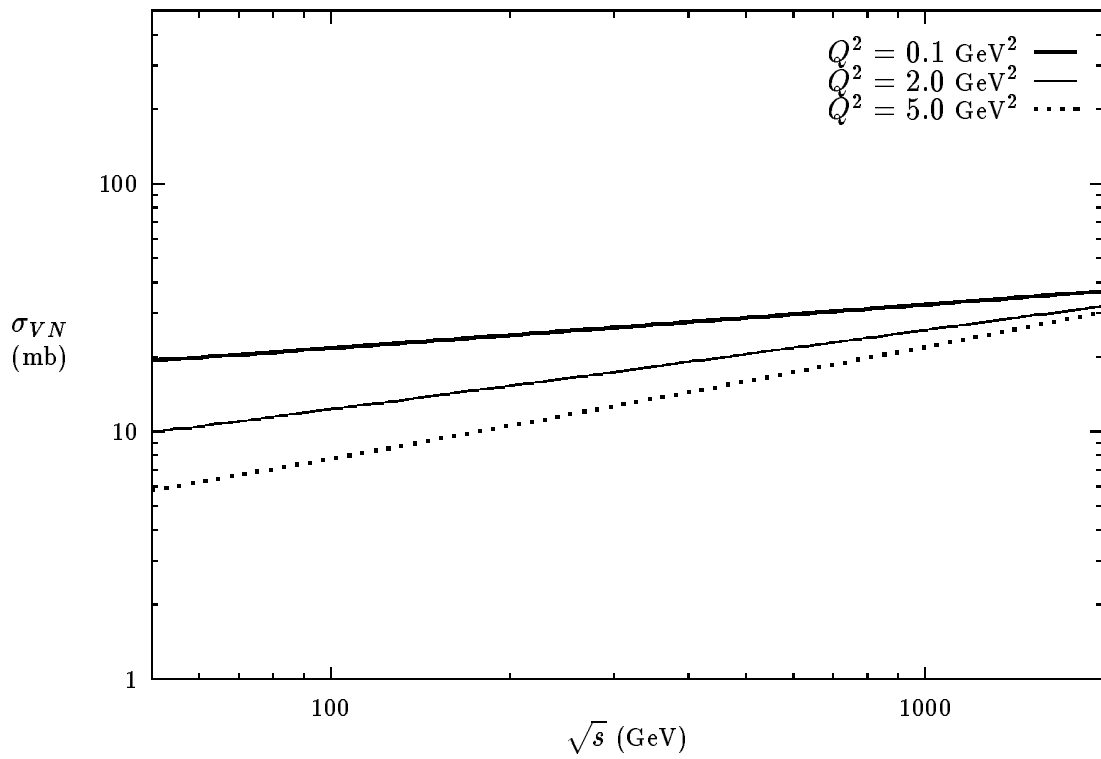
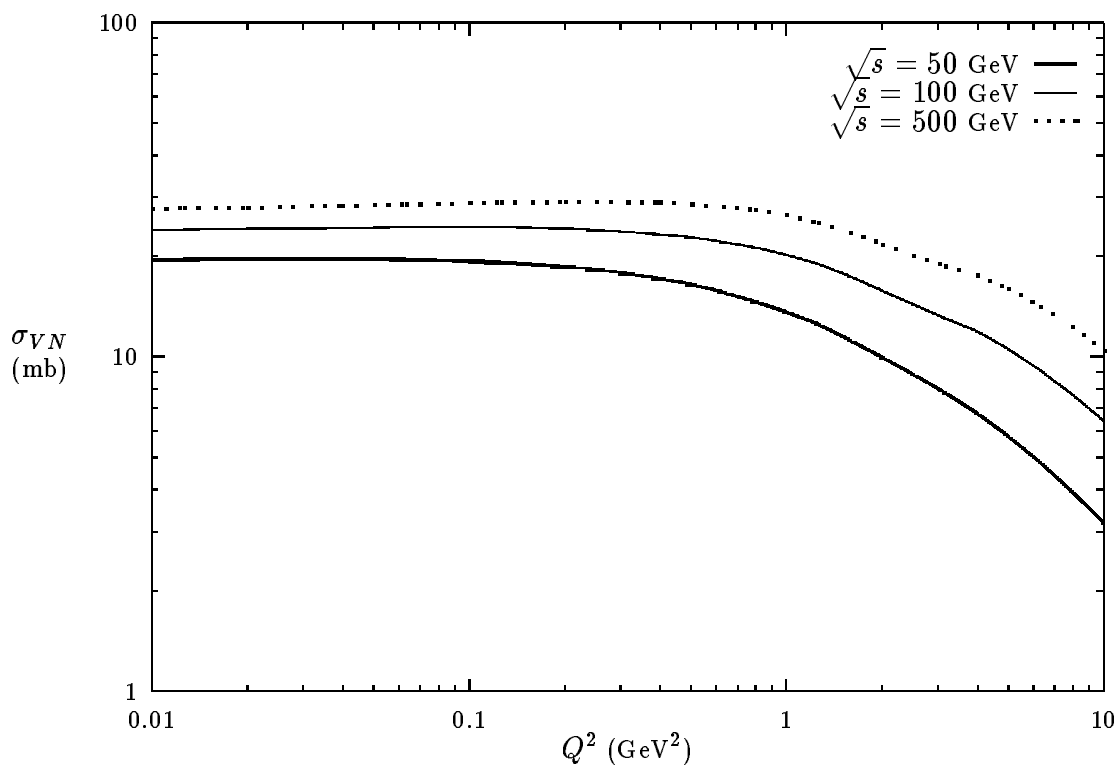


Fig. 1

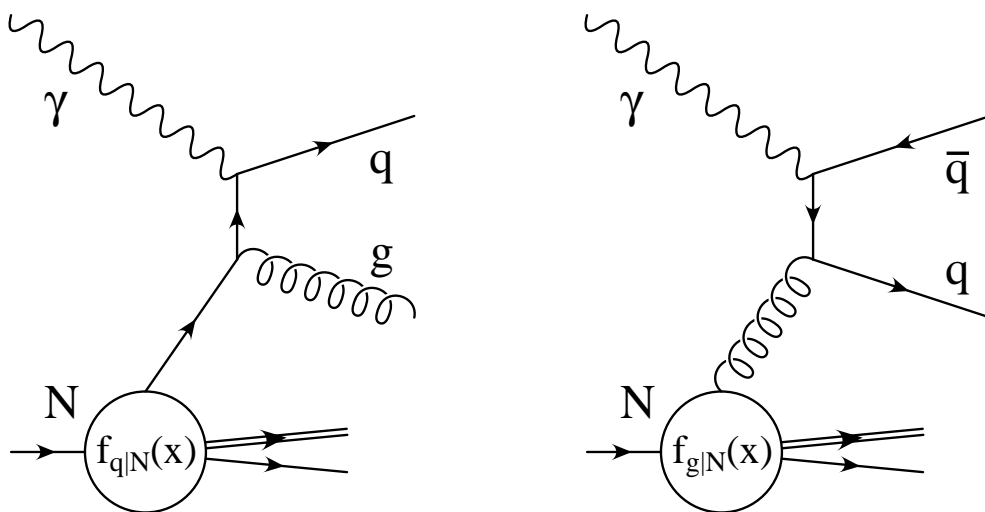


a)

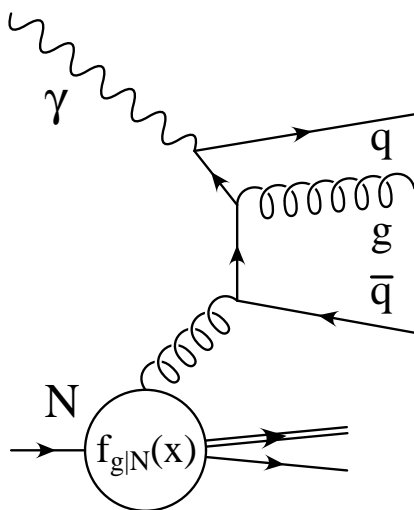


b)

Fig. 2



a)



b)

Fig. 3

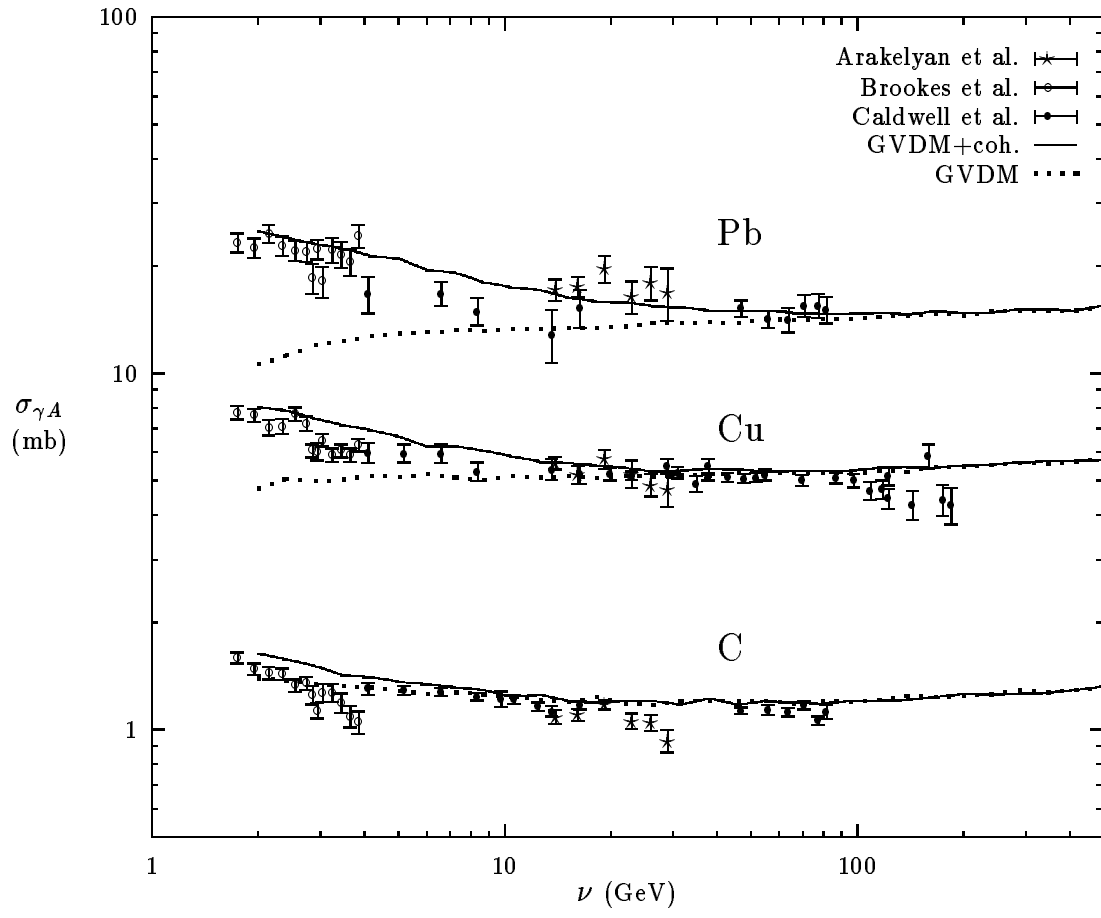


Fig. 4

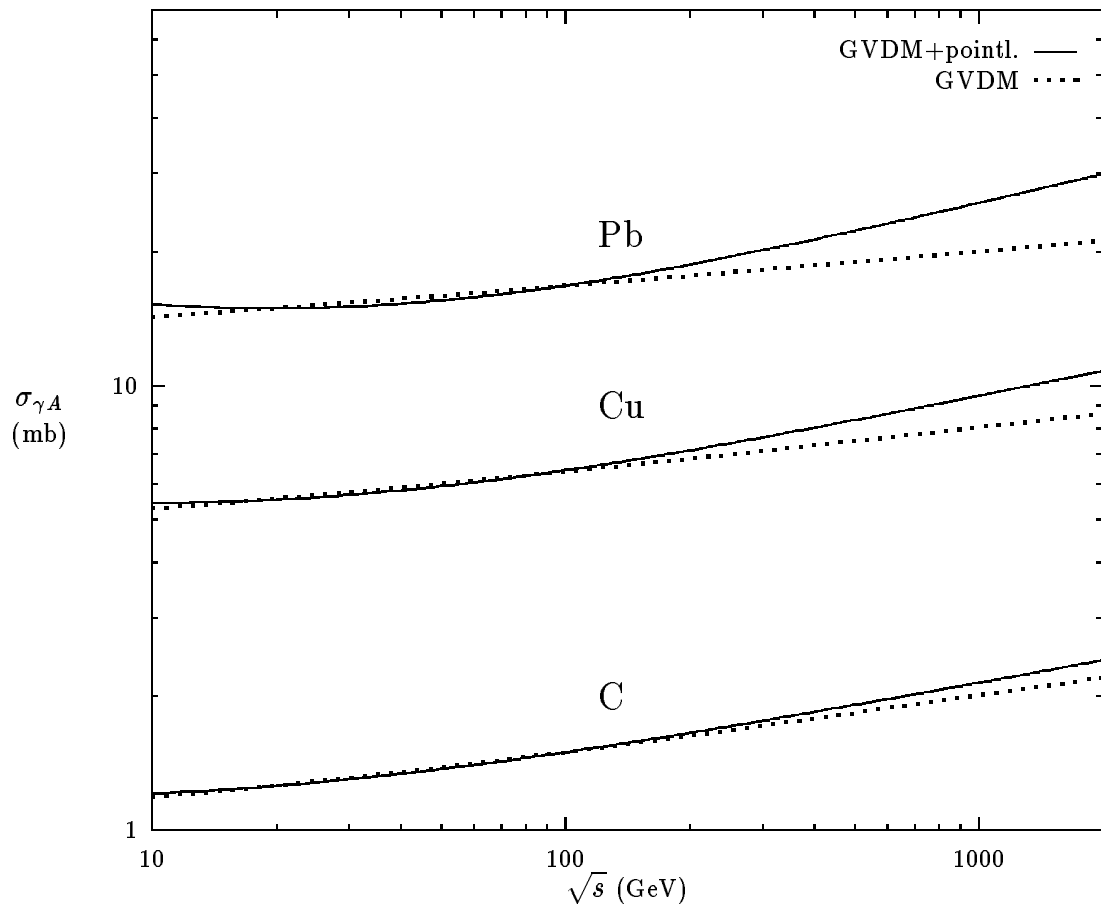
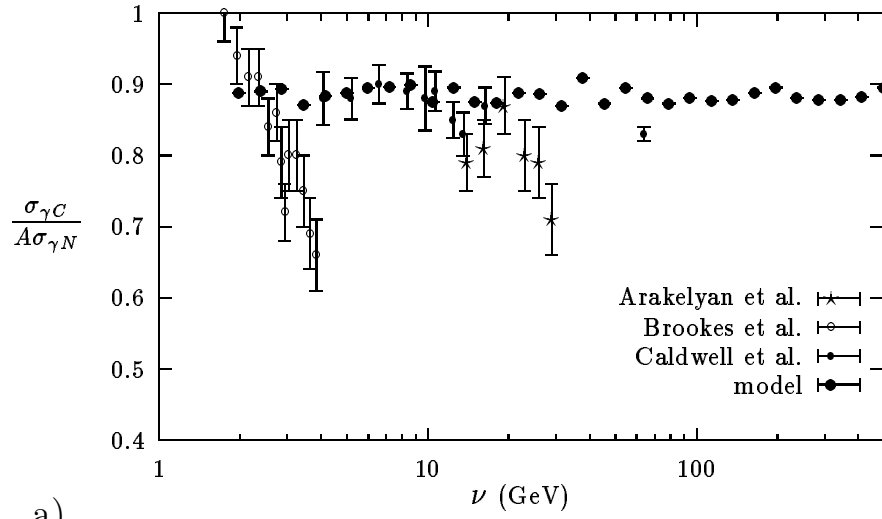
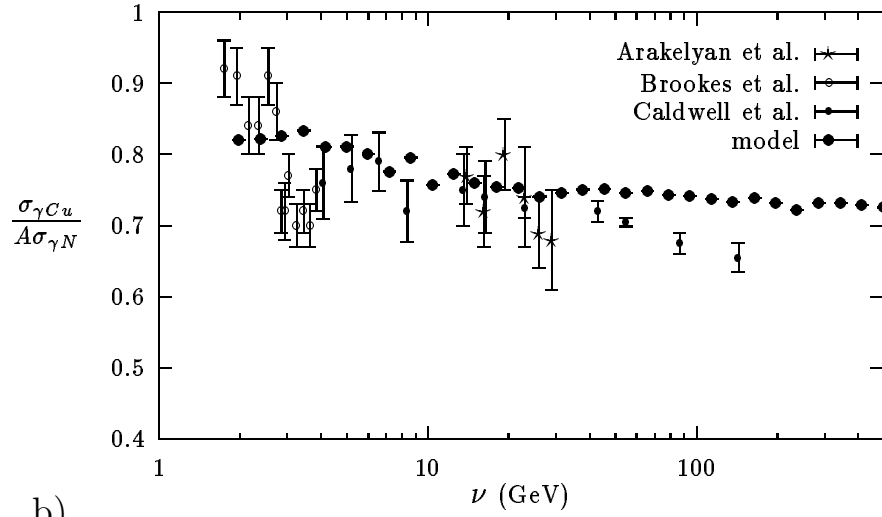


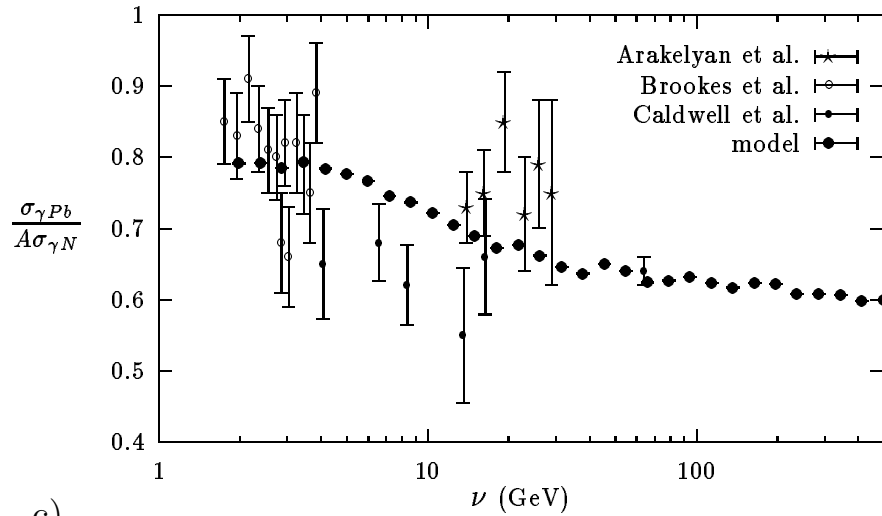
Fig. 5



a)



b)



c)

Fig. 6

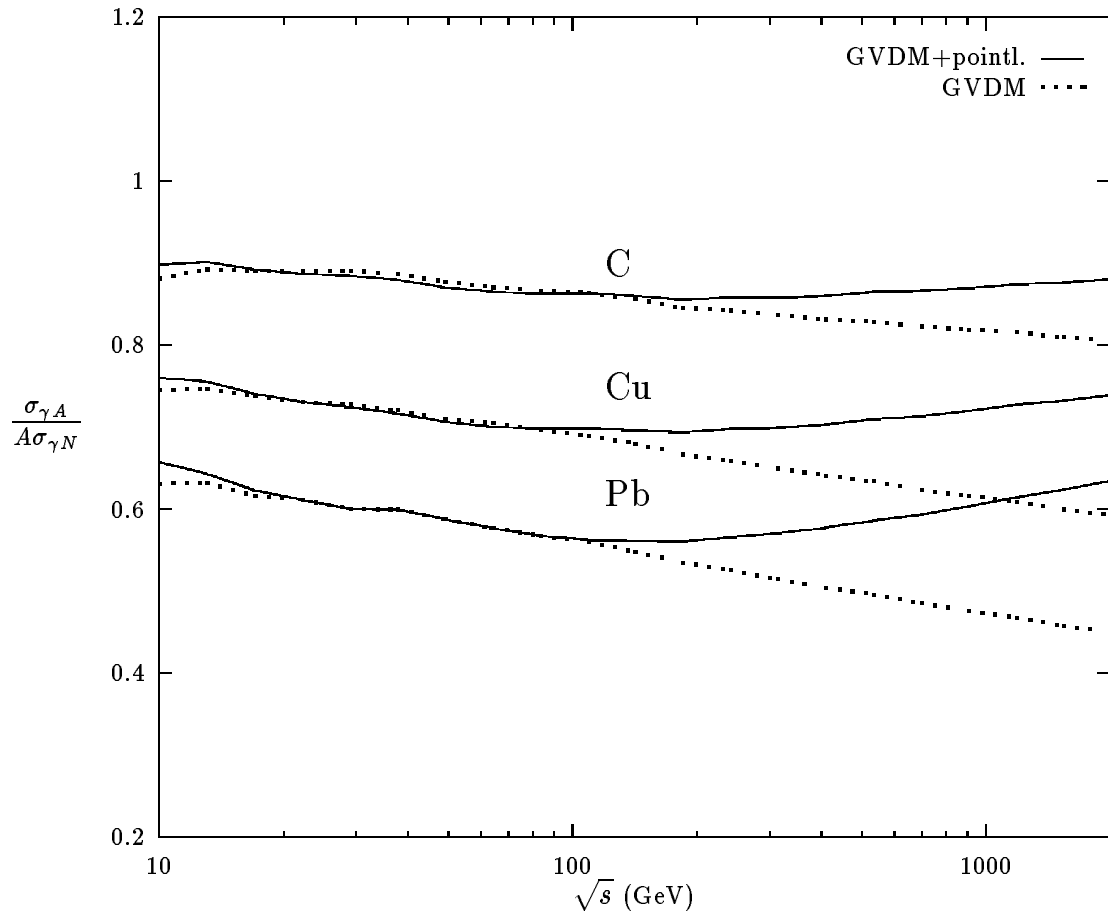


Fig. 7

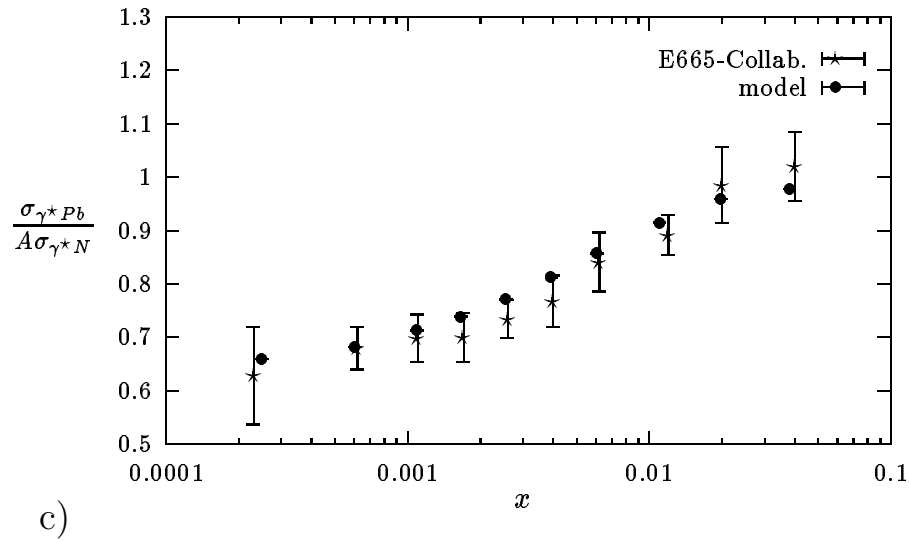
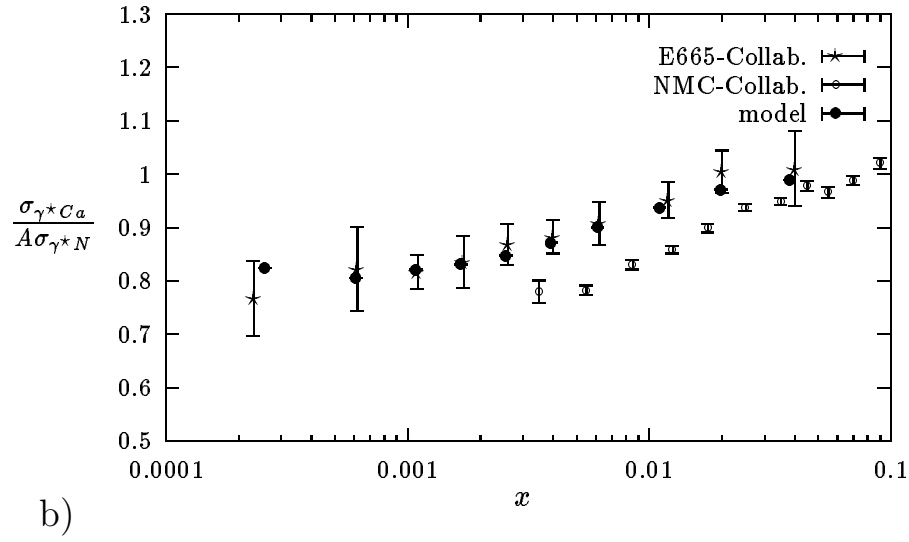
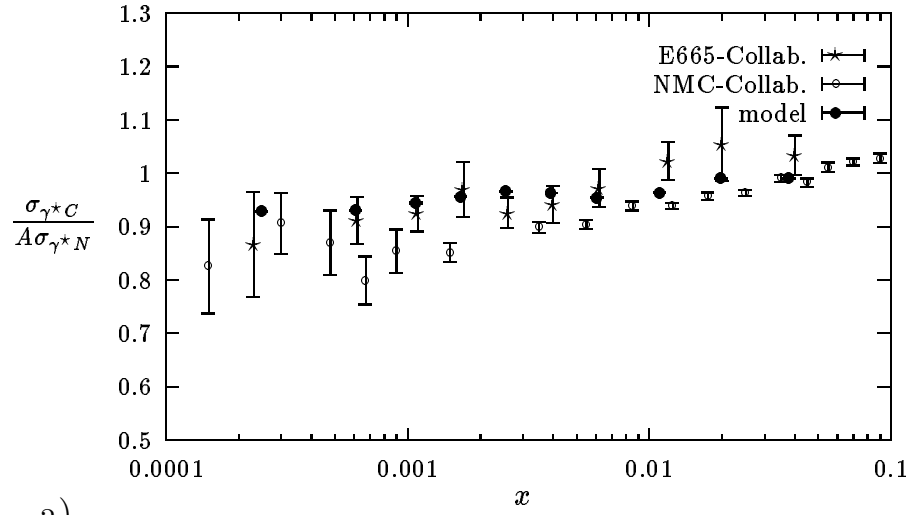
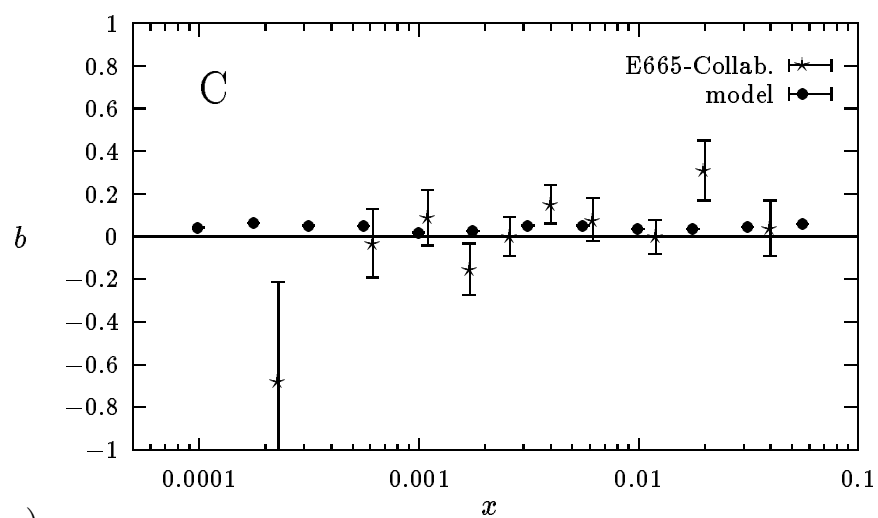
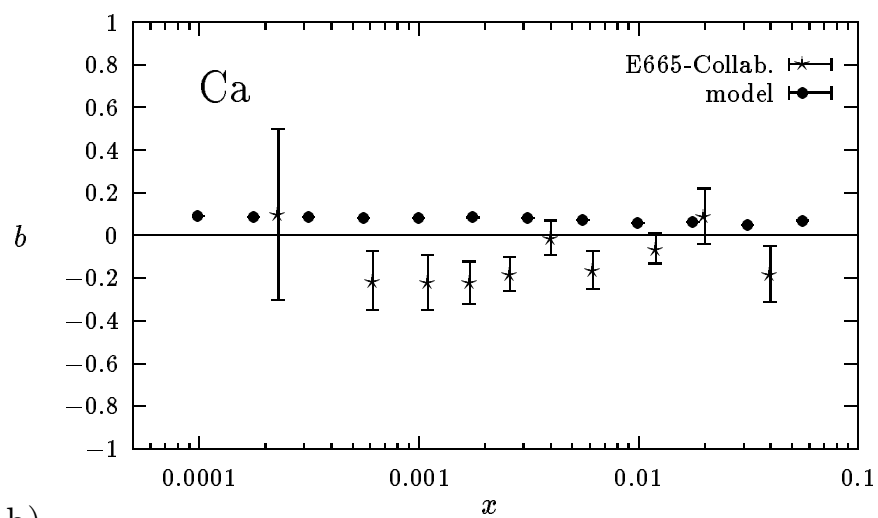


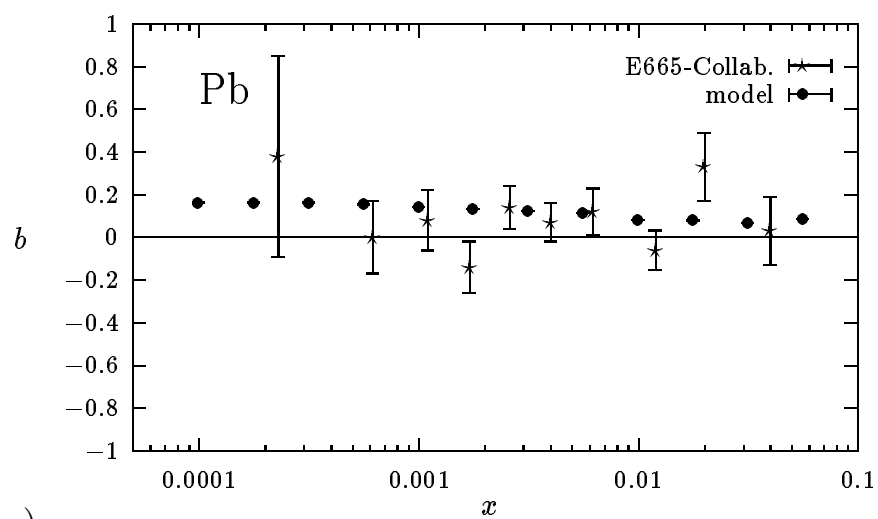
Fig. 8



a)



b)



c)

Fig. 9

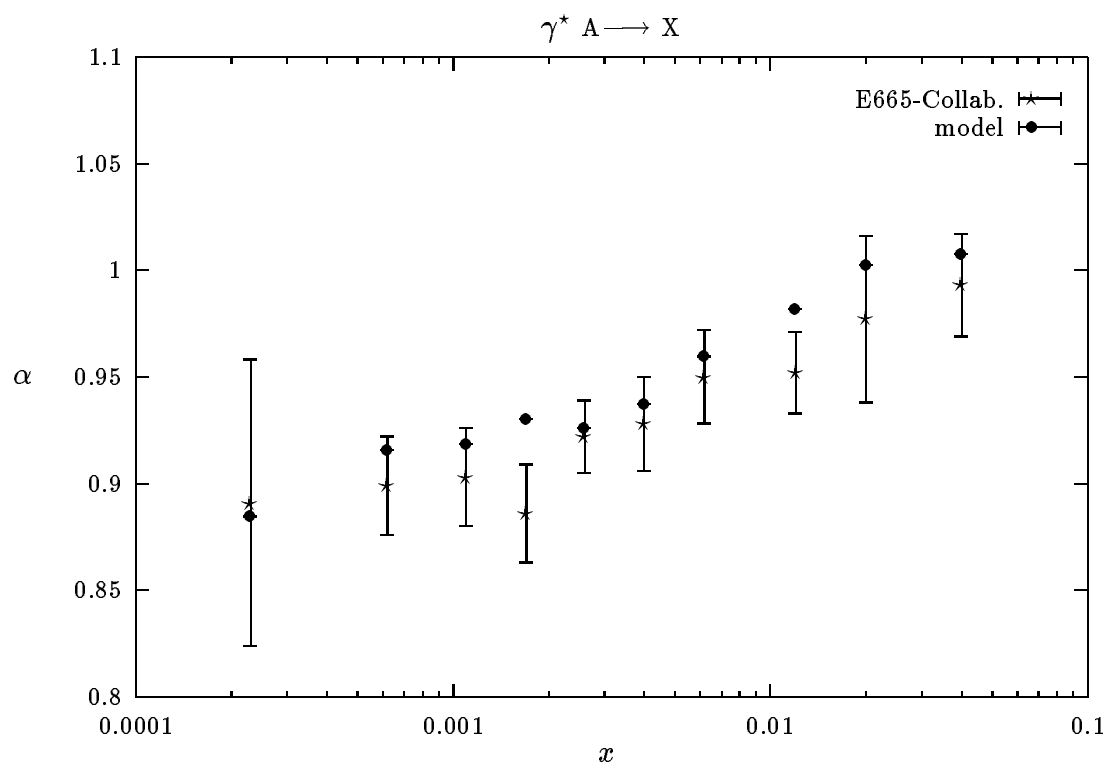
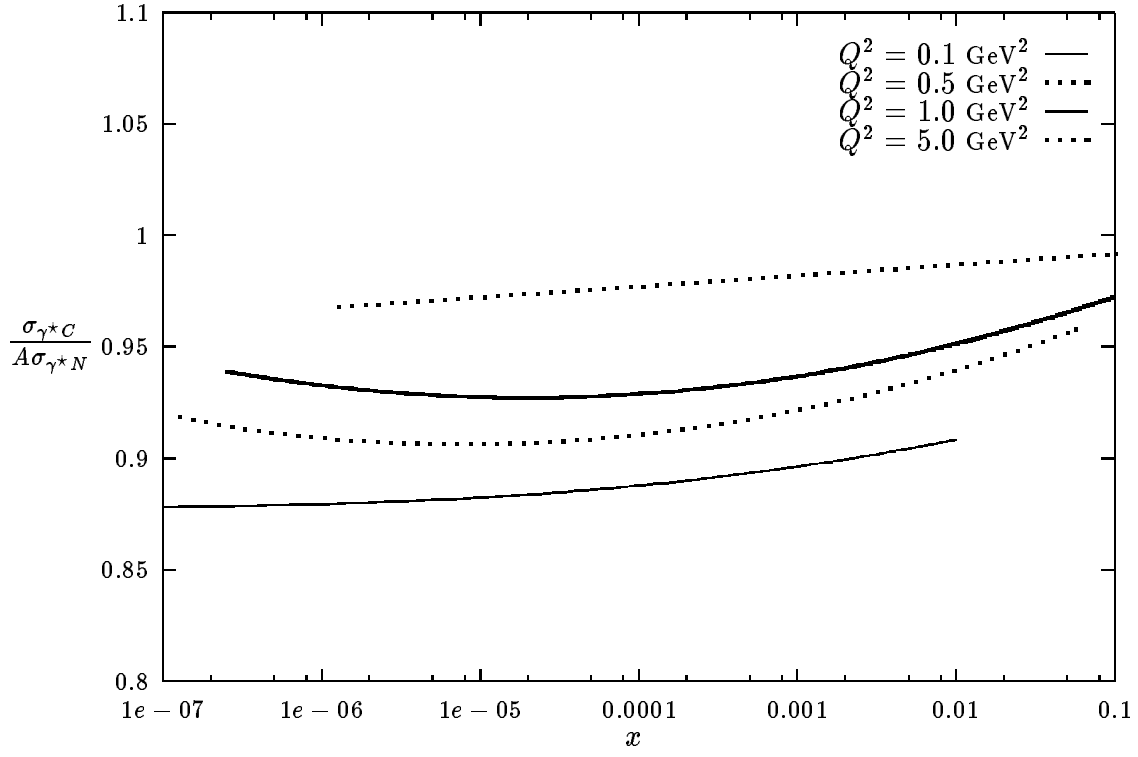
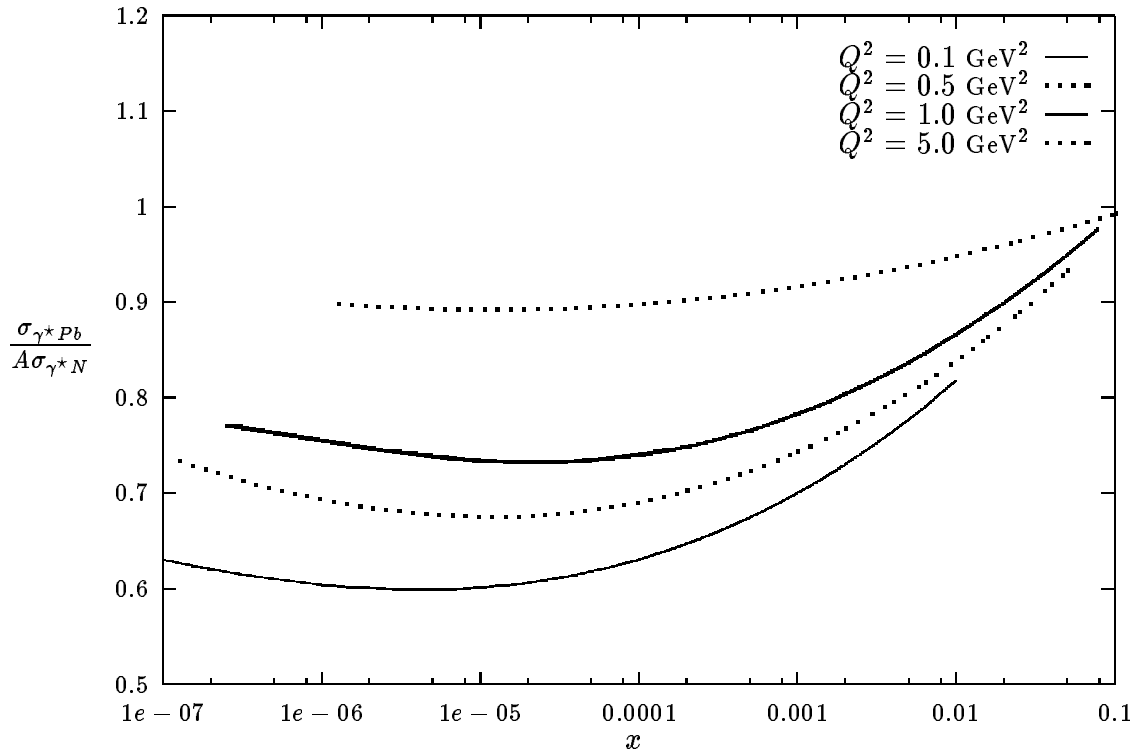


Fig. 10



a)



b)

Fig. 11

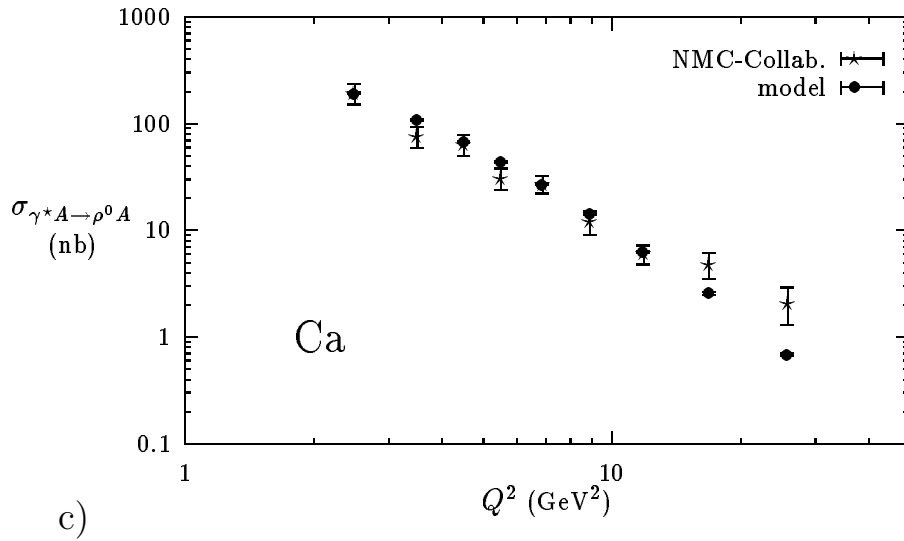
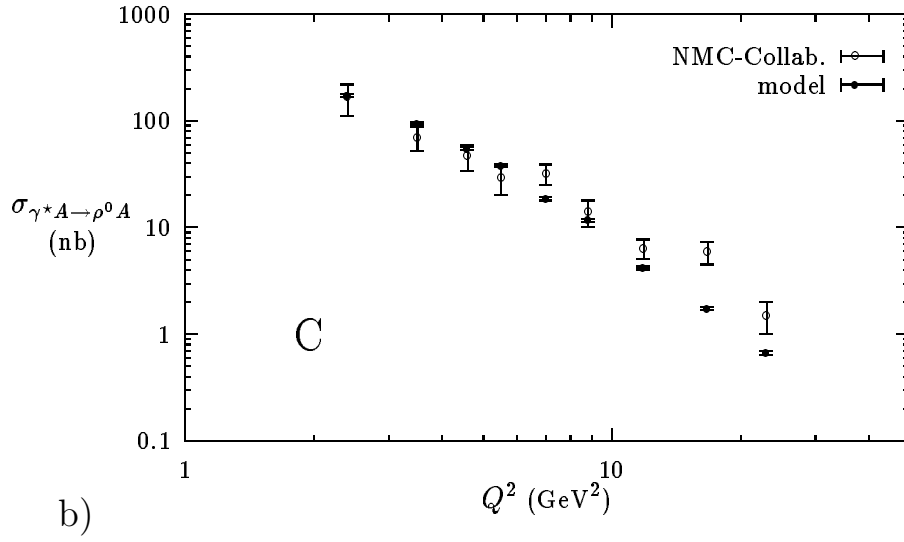
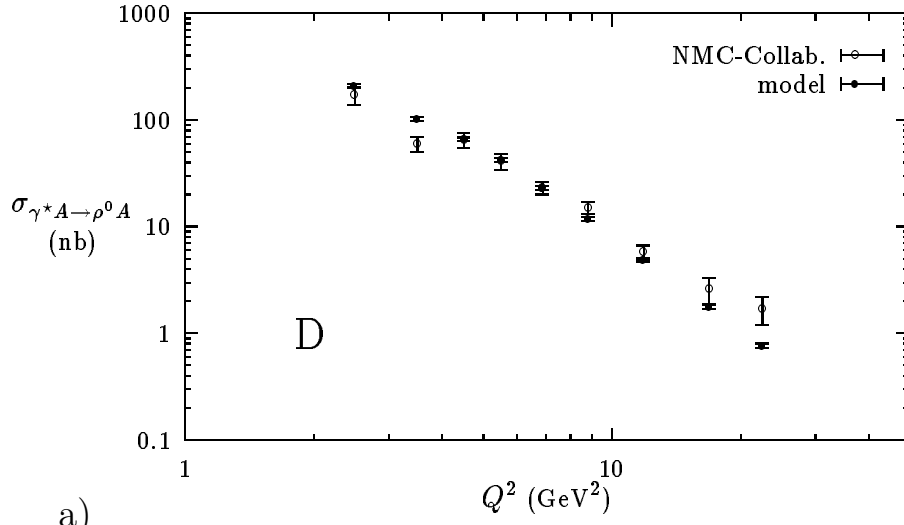


Fig. 12